

# RSC Advances



This is an *Accepted Manuscript*, which has been through the Royal Society of Chemistry peer review process and has been accepted for publication.

*Accepted Manuscripts* are published online shortly after acceptance, before technical editing, formatting and proof reading. Using this free service, authors can make their results available to the community, in citable form, before we publish the edited article. This *Accepted Manuscript* will be replaced by the edited, formatted and paginated article as soon as this is available.

You can find more information about *Accepted Manuscripts* in the [Information for Authors](#).

Please note that technical editing may introduce minor changes to the text and/or graphics, which may alter content. The journal's standard [Terms & Conditions](#) and the [Ethical guidelines](#) still apply. In no event shall the Royal Society of Chemistry be held responsible for any errors or omissions in this *Accepted Manuscript* or any consequences arising from the use of any information it contains.

**Thermal responsive behaviour of the electrical resistance of electrospun  
P(NIPAm-co-NMA)/Ag composite nanofibers**

Hui Li,<sup>a, b</sup> Guoping Zhang,<sup>a</sup> Libo Deng,<sup>\*a</sup> Rong Sun,<sup>\*a</sup> and Yangxing Ou<sup>b</sup>

<sup>a</sup>Shenzhen Institutes of Advanced Technology, Chinese Academy of Sciences,  
Shenzhen, 518055, China

<sup>b</sup>College of Materials Science and Engineering, Shenzhen University, Shenzhen,  
518060, China

**Abstract**

Thermal responsive copolymer P(NIPAm-co-NMA) was prepared via a radical copolymerization and spun into nanofibers using electrospinning. After thermal crosslinking, the electrospun fibers were modified using KH590 and silver nanoparticles were introduced onto the fiber surface using a chemical plating method. The electrical resistance of the composite fibers containing 65.5% of silver at different temperatures was investigated and it was found that the resistance dropped by ~60% as the temperature increased from 42 °C to 46 °C, which is consistent with the solubility transition of PNIPAm with the change of temperature as revealed by differential scanning calorimetry (DSC) measurement.

---

\* Corresponding authors: Denglb@siat.ac.cn and Rong.sun@siat.ac.cn; Tel: +86-0755-86392158

## 1. Introduction

Flexible sensors that can detect the change of temperature, strain/pressure and pH are essential components of wearable electronic devices which have been enjoying rapid growth recently.<sup>1-4</sup> Such sensors are mostly built on flexible/elastic substrates that show response to external stimuli. Fibers produced using an electrospinning technique is considered to be ideal substrates as the electrospun fibers with a typical diameter of hundreds of nanometers possess high surface areas, good mechanical properties and flexibilities.<sup>5</sup> Electrospun fibrous mats have been used for a range of sensors such as strain and gas sensors.<sup>6-8</sup> For example, Park *et al.* prepared elastomeric fibers containing silver nanoparticles using electrospinning and the electrospun fibers showed very high sensitivity to pressure at large deformations.<sup>9</sup> Tremendous efforts have been devoted to strain/pressure (human motion) and gas sensing so far,<sup>6-8, 10</sup> but there are few reports on using electrospun fibers as temperature sensors.<sup>11</sup>

Poly(N-isopropylacrylamide) (PNIPAm), as a typical thermoresponsive polymer, has been studied extensively in the last decades for potential applications in sensing and drug delivering.<sup>12-15</sup> The polymer chain in an aqueous solution shrinks dramatically as the temperature exceeds the lower critical solution temperature (LCST, which is 32 °C for neat PNIPAm),<sup>16, 17</sup> which can lead to a dramatic change of the

electrical properties when conductive fillers are embedded in, or attached to, the polymer matrix.<sup>18, 19</sup> The response of volume and electrical resistance to the temperature is even more pronounced when the polymer is in the form of nanofibers. However, the water-soluble homopolymer need to be modified to maintain the fiber integrity in an aqueous environment. There are generally two strategies, *i.e.* copolymerization with other monomers and non-covalently mixing with water-insoluble polymers,<sup>20-22</sup> to stabilize PNIPAm nanofibers.

In the present study, NIPAm and N-methylol acrylamide (NMA) monomers were copolymerized in which the NMA provides the thermal crosslinking function for the copolymer. Nanofibers of the copolymer were fabricated by electrospinning and followed by thermal crosslinking. The fiber surface was modified with a coupling agent 3-mercaptopropyltrimethoxysilane (KH590) on which the thiol group provides strong adhesion with metals. Silver nanoparticles were then introduced onto the fibers using a chemical plating method and the resistance of the composite nanofibers was measured at different temperatures. These fibers might find potential applications in temperature sensors due to their excellent stability and the strong adhesion between the fiber and the conductive particles.

## 2. Experimental

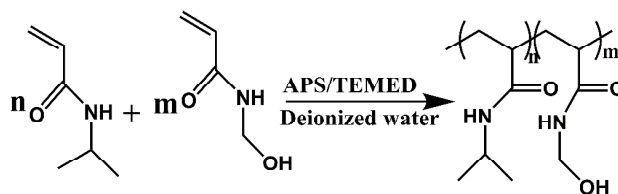
### 2.1. Materials

NIPAM, NMA, ammonium persulfate (APS), *N,N,N',N'*-tetramethylethylenediamine (TEMED), silver nitrate ( $\text{AgNO}_3$ ), sodium hydroxide (NaOH), ammonium hydroxide ( $\text{NH}_4\text{OH}$ ), glucose, nitric acid ( $\text{HNO}_3$ ), DMF, THF, ethanol, n-hexane, chloroform and acetic ether were purchased from Aladdin Reagent Co. Ltd (China). The monomer NIPAM was purified by recrystallization from n-hexane and NMA was purified by recrystallization from chloroform. The initiator APS was purified by recrystallization from ethanol. The other chemicals were used as received without further purification.

### 2.2. Synthesis of poly(NIPAm-co-NMA)

P(NIPAm-co-NMA) was prepared via radical copolymerization following the methods reported in literatures.<sup>23,24</sup> The preparation procedure is shown in Scheme 1. NIPAm (2 g, 90 mol%) and NMA (0.198 g, 10 mol%) were added to a 100 mL three necked flask with a stir bar. 50 mL of deionized water was added after degassing and backfilling with nitrogen for four times. APS (2 wt% of total monomer) was dissolved in 2 mL deionized water and added into the flask under stirring. TEMED (5 wt% of total monomer) was then added to the flask slowly. Polymerization was carried out at 0 °C for the first 4 h and then at room temperature (25 °C) for 20 h. The resulting

solution was dialyzed against deionized water for 72 h to remove unreacted monomers. During this period, the deionized water was replaced every 12 h. The final dialysis product was freeze-dried by using a freeze-dryer attached to a vacuum pump.



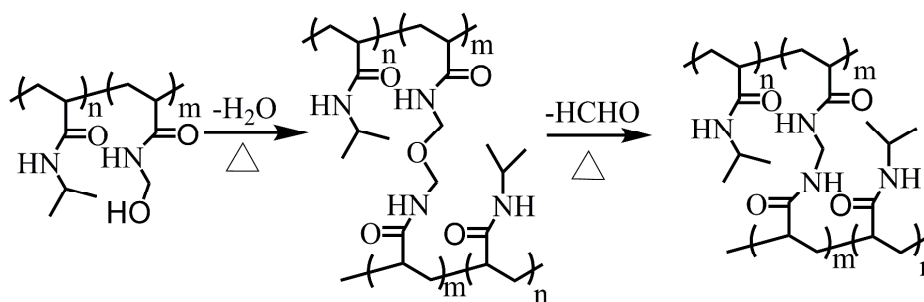
Scheme 1 The synthesis procedure of P(NIPAm-co-NMA) copolymer.

### 2.3. Electrospinning

P(NIPAm-co-NMA) was dissolved in DMF/THF (1:1) by stirring for 12 h at room temperature to form a stable solution with a concentration of 20%. The solution was loaded in a 12 mL syringe with a metal needle of 0.6 mm inner diameter. Electrospinning was then carried out using the conditions as follows: a flow rate of at  $1.2 \text{ mL h}^{-1}$ , a voltage of 10 kV and a tip-to-collector distance of 15 cm.

### 2.4. Crosslinking and surface modification of the fibers

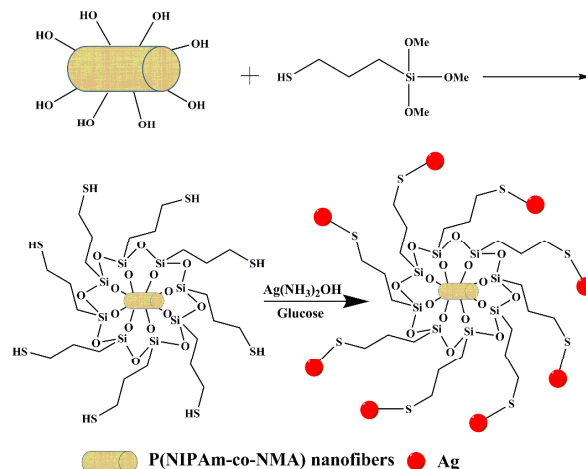
The electrospun nanofibers were baked at  $130 \text{ }^\circ\text{C}$  for 10 h for thermal crosslinking of NMA. The post-thermal-crosslinking reaction procedure is illustrated in Scheme 2.



Scheme 2 Schematic illustration of the crosslinking reaction.<sup>24</sup>

The thermal crosslinked poly(NIPAm-co-NMA) fibrous mat was washed in a NaOH solution with a concentration of 8 g L<sup>-1</sup> at 40 °C for 20 min to remove the residual small organic molecules and increase the hydrophilicity. The fibers were then rinsed with deionized water and ethanol and dried at 60 °C for 10 min. Silver nanoparticles were introduced onto the fiber following the procedure shown in Scheme 3. The mat was firstly immersed in an acetic ether solution of KH590 for 120 min and washed by ethanol for three times and then dried at 60 °C for 15 min. The KH590–modified P(NIPAm-co-NMA) fibrous mat was then immersed in a silver plating solution with constant stirring for metallising reaction. Two solutions were prepared separately and mixed in the metallising bath before plating. One was a silver ion solution (solution A) and the other is a reducing agent solution (solution B). The composition of solution A was: AgNO<sub>3</sub>, NaOH (0.25 g L<sup>-1</sup>), NH<sub>4</sub>OH (28 wt%) and that of solution B was: glucose, HNO<sub>3</sub> (2 g L<sup>-1</sup>) and ethanol (100 mL L<sup>-1</sup>). The concentration of AgNO<sub>3</sub> (the molar ratio of AgNO<sub>3</sub> to glucose was 1:1) was 0.01 mol L<sup>-1</sup>, 0.05 mol L<sup>-1</sup> and 0.1 mol L<sup>-1</sup>, and the resultant fibers are denoted as

PNN/Ag-0.01, PNN/Ag-0.05 and PNN/Ag-0.1, respectively. After plating, the fibrous mats were cleaned in deionized water and dried at 60 °C for 24 h.



Scheme 3 Schematic illustration of the modification procedure of the P(NIPAm-co-NMA).

### 2.5. Characterization of poly(NIPAm-co-NMA)/Ag composite nanofibers

Proton nuclear magnetic resonance ( $^1\text{H-NMR}$ ) spectra were obtained on a 400 MHz NMR spectrometer and dimethyl sulfoxide- $d_6$  (DMSO- $d_6$ ) was used as the solvent. The fiber morphology was investigated using field-emission scanning electron microscope (FE-SEM, FEI Nova Nano SEM 450) equipped with an energy dispersive X-ray spectrometer (EDS) after gold coating. The diameter of the fibers and Ag particles were determined using an Image J software from high-magnification SEM images (see Fig. S1 in the Electronic Supplementary Information). To measure the LCST, the nanofibers were wetted by water for 24 h and put into DSC cells. DSC thermograms were then obtained at a heating rate of  $5\text{ }^\circ\text{C min}^{-1}$  from  $10\text{ }^\circ\text{C}$  to  $70\text{ }^\circ\text{C}$



using a TA Q20 (USA) System. The LCST was defined as the onset value of transition temperature chart. Thermogravimetric analysis (TGA) was carried out at a heating rate of  $10\text{ }^{\circ}\text{C min}^{-1}$  from  $100\text{ }^{\circ}\text{C}$  to  $800\text{ }^{\circ}\text{C}$  using a TA Q600 (USA) system. The electrical resistance was measured at different temperatures using a multimeter (Fluke, USA). Electrodes were attached directly to the fibrous mat saturated with water and the separation of the electrodes was set at 1 cm for all measurements. The temperature was increased using a hot stage from  $30$  to  $54\text{ }^{\circ}\text{C}$  with a step of  $2\text{ }^{\circ}\text{C}$ . The mats were stabilized for 10 min at each temperature before the measurement was performed.

### 3. Results and discussion

#### 3.1. Characterization of P(NIPAm-co-NMA)

Fig. 1 shows the  $^1\text{H-NMR}$  spectrum of the P(NIPAm-co-NMA) copolymer in DMSO- $d_6$ . The methylene group, the methine of PNIPAm and NMA protons overlap each other and appear at  $\delta = 2.0$  (peak a) ppm and  $\delta = 1.5$  ppm (peak b), respectively. The  $-\text{NH}$  resonances of the PNIPAm and NMA units appear at  $\delta = 7.25$  ppm (peak c) and  $\delta = 8.0$  ppm (peak c'), respectively. The methine of PNIPAm protons appear at  $\delta = 3.85$  (peak d) ppm. The  $(-\text{CH}_3)$  of PNIPAm protons appear at  $\delta = 1.10$  ppm (peak e). The methylene group of NMA protons appear at  $\delta = 4.5$  (peak f) ppm. The  $(-\text{OH})$

proton resonances of NMA appear at  $\delta = 5.49$  ppm (peak g). These results are consistent with those reported in the literature for P(NIPAm-co-NMA),<sup>23</sup> suggesting that the copolymer has been successfully synthesized.

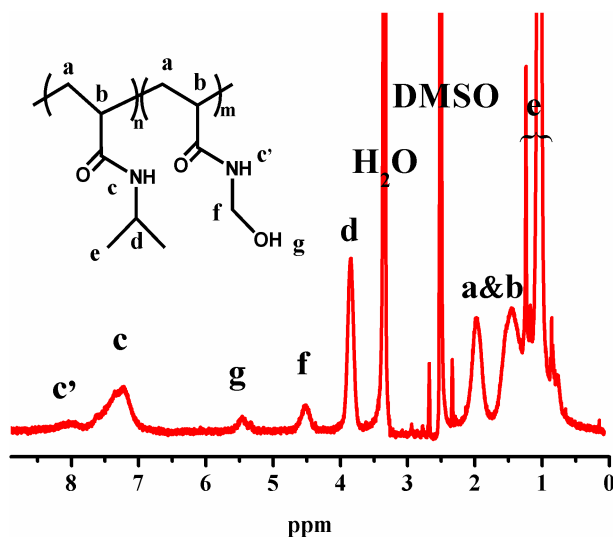


Fig. 1 <sup>1</sup>H-NMR spectrum of the P(NIPAm-co-NMA) copolymer.

### 3.2. The morphology of P(NIPAm-co-NMA) nanofibers

P(NIPAm-co-NMA) nanofibers were fabricated by electrospinning and an SEM image of the fibers is shown in Fig. 2a. It can be seen the electrospun P(NIPAm-co-NMA) fibers possess smooth, uniform and beadless surfaces with an average diameter of 410 nm. The as-prepared fibers are water-soluble at room temperature which hinders their practical applications. Crosslinking the fiber might decrease the solubility and increase the water-resistance. The fibers were thus baked at 130 °C for 10 h and the SEM image is shown in Fig. 2b. It can be seen that the fiber diameter and morphology are unaffected upon the heat treatment.

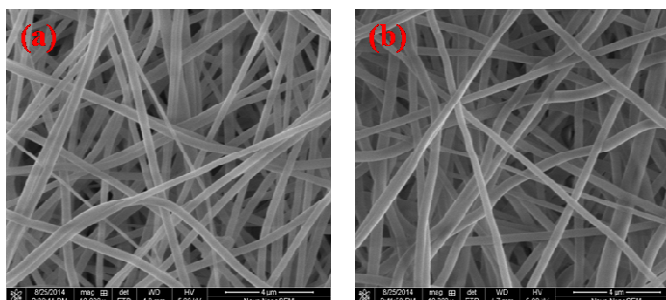


Fig. 2 SEM images of (a) the as-prepared and (b) the heat-treated P(NIPAM-co-NMA) fibers.

### 3.3. Modification of the electrospun fibers

Figs. 3a and 3b show the  $^1\text{H-NMR}$  spectra of the as-prepared and the heat-treated P(NIPAm-co-NMA) fibers. It can be seen that the peak at 5.49 ppm which corresponds to the  $-\text{OH}$  group of NMA in the pristine fibers is reduced after baking at  $130\text{ }^\circ\text{C}$  for 6 h. This suggests the loss of OH group and crosslinking of the copolymer (also confirmed by FTIR characterization, see Fig. S2), which might enhance the stability of the fibers in an aqueous environment. The degree of crosslinking can be quantitatively characterized by the ratio between the integration of 5.49 ppm peak ( $-\text{OH}$  proton) and that of 3.85 ppm peak ( $-\text{CH}$  proton). The  $I_{\text{OH}}/I_{\text{CH}}$  ratio as functions of the curing temperature and time are shown in Fig. S3. It is found that with the increase of curing temperature and time the ratio decreases. The  $I_{\text{OH}}/I_{\text{CH}}$  ratio for the fibers treated at  $130\text{ }^\circ\text{C}$  for 6 h is approximately 18% of the initial value, suggesting an 82% of crosslinking. The fibers treated at  $130\text{ }^\circ\text{C}$  for 10 h is insoluble and thus the NMR spectrum is not shown here. However, there are still hydroxyl groups remaining

after heat treatment (and particularly after the NaOH pretreatment), which provides active sites for further modification.

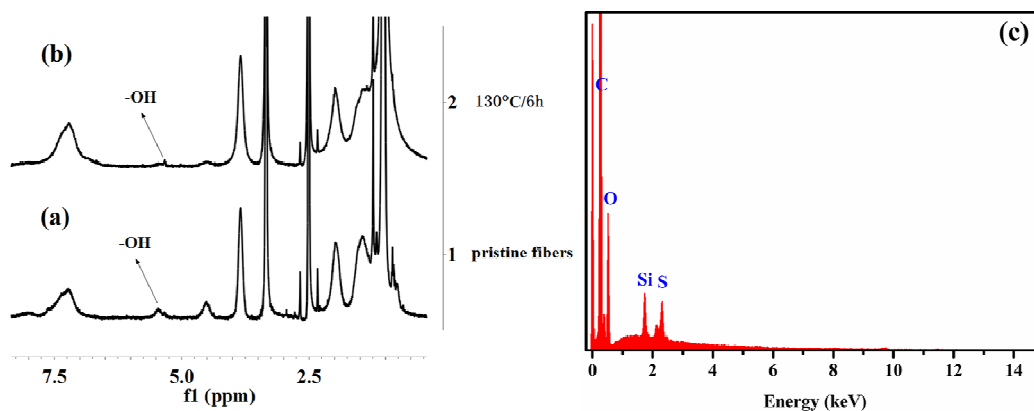


Fig. 3 (a) and (b) <sup>1</sup>H-NMR spectra of the as-prepared and the crosslinked P(NIPAM-co-NMA) fibers; (c) the EDS spectrum of the modified P(NIPAm-co-NMA) fibers.

Conductive particles can be incorporated into a polymer matrix by direct blending, in situ polymerization and other methods. In this study, we used a strategy shown in Scheme 3 to introduce silver onto the fiber surface. The silver coating layer that adheres strongly to the polymer endows the polymer with a high conductivity. To this end, the crosslinked P(NIPAm-co-NMA) fibrous mat was firstly modified with KH590 through condensation reaction between the methoxy of KH590 and the remaining hydroxyl of the crosslinked P(NIPAm-co-NMA) fibers. The EDS spectrum of the modified P(NIPAm-co-NMA) nanofibers which had been washed in ethanol for three times is shown in Fig. 3c. Silicon (Si) and sulfur (S) were found from the fibers, which suggests the successful modification of the fibers by the coupling agent. Silver

was then introduced onto the fiber surface by chelation reaction with the thiol group of KH590. Such reaction provides strong adhesion between silver and the fiber.<sup>25</sup> The silver coating layer did not fall off even after 20 mins' ultrasonication. The loadings of silver in fibers plated in the  $\text{AgNO}_3$  solution with concentrations of 0.01, 0.05 and  $0.1 \text{ mol L}^{-1}$  are 4.2%, 41.1% and 65.5%, respectively, as revealed by the TGA curves shown in Fig. 4. It should be noted the weight percent of silver was determined taking into account of the residue (<2.6%) derived from the polymer in the composite fibers. Fibers with different molar fractions of NMA were plated in the  $0.01 \text{ mol L}^{-1} \text{ AgNO}_3$  solution and it was found the loading of silver increases with the increase of the NMA fraction as can be seen from Fig. S4. This suggests stronger interactions between the fiber and silver at a higher NMA fraction.

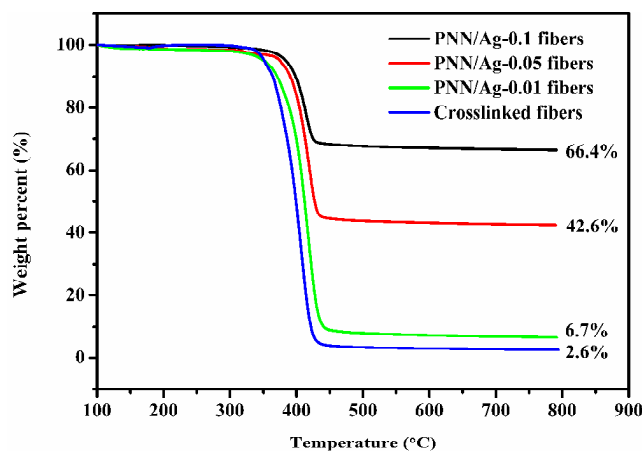


Fig. 4 TGA curves of the crosslinked P(NIPAM-co-NMA) fibers and P(NIPAM-co-NMA)/Ag composite fibers.

### 3.4. Fiber mat integrity

As mentioned above, one of the major challenges in using PNIPAm-based smart nanofibers is the stability of the polymer in aqueous media below the LCST.<sup>23</sup> Fig. 5 shows digital images of the pristine and crosslinked fibers both below and above the LCST. The crosslinked fibers retain the fibrous morphology in water whereas the pristine fibers dissolve in water within a few minutes at room temperature. While above the LCST, both fibers remain intact but the mats shrink significantly due to the perturbation of hydrogen bonding with water.

The integrity of the crosslinked fiber can be quantified by leaching experiments. The vacuum-dried fibers were soaked in water and heated to 50 °C and then cooled down to room temperature. The fibers were then thoroughly dried and the weight was recorded. It was noticed that after five cycles of heating and cooling, the weight of the fibrous mat reached a constant value, of similar to 98% of the initial value. The fibrous morphology was also retained after the repeated heating and cooling cycles, which suggests excellent stability of the crosslinked fibers.

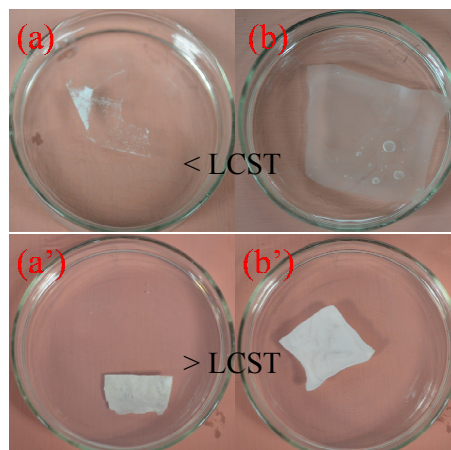


Fig. 5 Digital images of (a and a') the pristine and (b and b') the crosslinked fibers both below and above the LCST.

### 3.5. Characterization of P(NIPAm-co-NMA)/Ag composite fibers

Fig. 6 and Fig. S5 show SEM images of the P(NIPAm-co-NMA)/Ag composite fibers plated in  $\text{AgNO}_3$  solutions with different concentrations. The composite fibers swelled slightly upon plating. For the PNN/Ag-0.01 fiber, (the concentration of  $\text{AgNO}_3$  in the plating solution was  $0.01 \text{ mol L}^{-1}$ ), silver particles were uniformly distributed on the fiber surface (Fig. 6a). The average diameter of silver particles was 10 nm and the interparticle separation was large due to the low total volume of the particles. As the concentration of  $\text{AgNO}_3$  increased to  $0.05 \text{ mol L}^{-1}$ , the average diameter of silver particles increased to 70 nm, the amounts of deposited silver nanoparticles increased significantly, and the particles contacted each other (Fig. 6b). At low concentrations of  $\text{AgNO}_3$ , the silver seeds are generated inadequately and the

seeds grow slowly, which result in small particle size. As the concentration of  $\text{AgNO}_3$  increased further to  $0.1 \text{ mol L}^{-1}$ , the surfaces of the polymer fibers were fully covered by silver particles as shown in Fig. 6c (primary silver particles indistinguishable). The average diameter of silver nanoparticles increases with the increase of  $\text{AgNO}_3$  concentration, due probably to the fast self-nucleation of silver nanoparticles at high concentrations of  $\text{AgNO}_3$  and the high reduction rate of silver ions at high concentrations of glucose solution.<sup>26</sup>

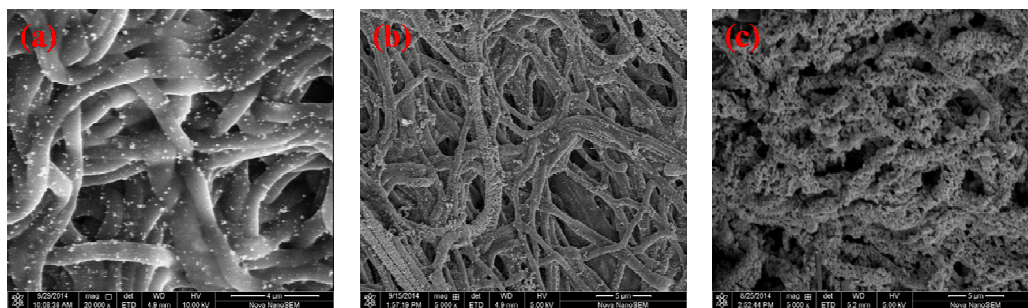


Fig. 6 SEM images of (a) PNN/Ag-0.01, (b) PNN/Ag-0.05 and (c) PNN/Ag-0.1 fibers.

### 3.6. The thermo-switchable electrical resistance of the composite fibers

The electrical resistances of the fibrous mats measured at different temperatures are shown in Fig. 7 (the resistances  $R_i$  at different temperatures were normalized to the initial value  $R_0$  measured at  $30 \text{ }^\circ\text{C}$ ). For the PNN/Ag-0.01 fibers, the resistance remains almost constant with the increasing temperature, which is thought to be associated with the low density of conductive particles in the film.<sup>18</sup> The shrinking of the composite film is insufficient to bring the sparsely-distributed silver particles into



contact with each other in this case. As for the PNN/Ag-0.05 fibers, the resistance decreases gradually with the increasing temperature due to change of the volume of the fibrous mat, showing a low temperature sensitivity.<sup>27</sup> This is possibly associated with the low volume fraction of silver in the composites.

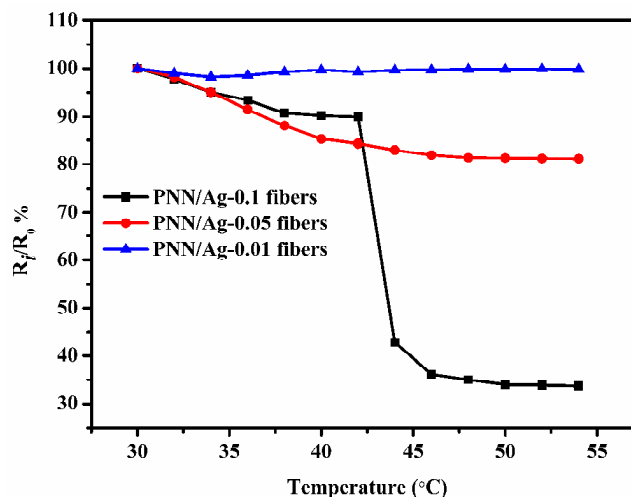


Fig. 7 The dependence of resistance on the temperature for the composite fibers.

The resistance of the PNN/Ag-0.1 fibers decreased slightly with the increase of temperature in the range of 30-42 °C, a behaviour similar to that of PNN/Ag-0.05. However, as the temperature exceeded 42 °C, the resistance dropped by ~60% for a temperature change of only 4 °C, exhibiting a very high sensitivity to the change of temperature. The responsive behaviour observed from PNN/Ag-0.1 is in qualitative agreement with Ding's findings for a PNIPAm/gold nanoparticle composite hydrogel,<sup>18</sup> but is in contradiction to Chuang's findings, where a dramatic increase, *i.e.*

similar to 700% of the resistance increased within 20 °C was observed for P(NIPAM-co-NMA)/carbon black composite film.<sup>24</sup> However, the conductive fillers were embedded in the polymer matrix in Chuang's work whereas the silver particles were attached to the fibers surface in our case. The high sensitivity observed here is related to the transition from solvated random coils below the LCST to tightly packed globular particles above the LCST which originates from the breakdown of the hydrogen bonds between the polymer and water molecules.<sup>18</sup> As a result, the silver particles are packed at a higher density above the LCST and the resistance drops dramatically. Such a high sensitivity paves the way for flexible temperature sensor in the future although further work is needed to tailor the molecular structure of the copolymer and its LCST so that the sensor can work with high performance around 37 °C in biological systems. It should be noted that our parallel work on temperature sensor using a nonthermoreponsive polymer, phenoxy resin, as the matrix showed a much lower sensitivity, i.e. the resistance changed by 20% within 20 °C, which suggests the advantage of PNIPAm for temperature sensing application.

The temperature at which the resistance undergoes a dramatic drop is in excellent agreement with the transition temperature determined by DSC measurement which also suggested a LCST of 42 °C (Fig. 8). It is known the LCST for pure PNIPAm is similar to 32 °C, and increasing the hydrophilic of PNIPAm-based copolymer

generally leads to a higher LCST.<sup>28</sup> In our study, the hydrophilic NMA was introduced into the copolymer and the LCST was increased to 42 °C. An even higher LCST, of 48 °C, has been observed by Kim *et al.* from a P(NIPAm-co-NMA) copolymer.<sup>23</sup> As explained above, it is desired to tune the LCST further for practical applications, which remains our future work.

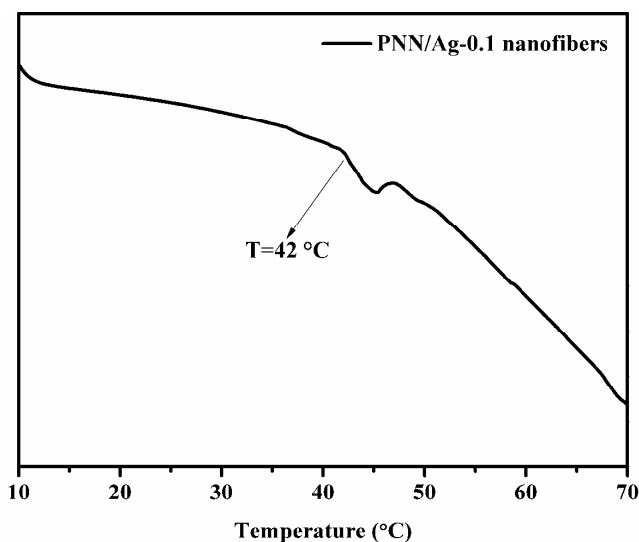


Fig. 8 The DSC curve of the wetted PNN/Ag-0.1 composite fibers.

#### 4. Conclusions

Through a radical copolymerization and electrospinning a thermal responsive nanofiber was prepared. After thermal crosslinking, the P(NIPAm-co-NMA) nanofibers were modified with KH590 and Ag nanoparticles was coated onto the fibers by using a chemical plating method. The crosslinked fiber mat showed excellent stability and strong adhesion with silver, which ensures the cyclic

performance of the fibers in an aqueous environment. For fibers containing silver higher than 41%, the electrical resistance of the fiber decreased slightly with the temperature below the LCST. While around the LCST, the resistance dropped by 60% for a temperature change of only 4 °C, exhibiting a very high sensitivity to the temperature. The approaches to stabilizing thermoresponsive fiber and modifying the fiber with conductive nanoparticles established in this study can be extended to preparing other responsive fibers, and pave the way for practical applications of electrospun fibers in flexible sensors.

### Acknowledgements

This work was supported by Guangdong and Shenzhen Innovative Research Team (Program No. 2011D052, KYPT20121228160843692), National Natural Science Foundation of China (Grant No. 21201175) and R&D Funds for basic Research Program of Shenzhen (Grant No. JCYJ20120615140007998).

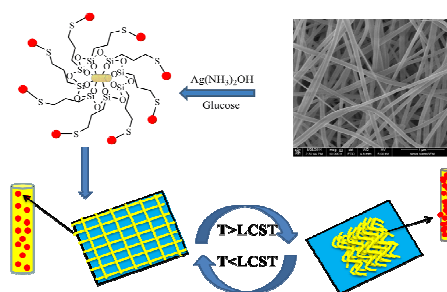
### References

1. K. Fukuda, Y. Takeda, Y. Yoshimura, R. Shiwaku, T. Lam Truc, T. Sekine, M. Mizukami, D. Kumaki and S. Tokito, *Nat Commun*, 2014, **5**, 4147.
2. W. Honda, S. Harada, T. Arie, S. Akita and K. Takei, *Adv. Funct. Mater.*, 2014, **24**, 3299-3304.
3. X. Liu, L. Gu, Q. Zhang, J. Wu, Y. Long and Z. Fan, *Nat Commun*, 2014, **5**, 4007.

4. M. R. Islam and M. J. Serpe, *RSC Adv*, 2014, **4**, 31937-31940.
5. B. Sun, Y.-Z. Long, Z.-J. Chen, S.-L. Liu, H.-D. Zhang, J.-C. Zhang and W.-P. Han, *J Mater Chem C*, 2014, **2**, 1209-1219.
6. J. S. Lee, O. S. Kwon, S. J. Park, E. Y. Park, S. A. You, H. Yoon and J. Jang, *Acs Nano*, 2011, **5**, 7992-8001.
7. L. Persano, C. Dagdeviren, Y. Su, Y. Zhang, S. Girardo, D. Pisignano, Y. Huang and J. A. Rogers, *Nat Commun*, 2013, **4**, 1633.
8. B. Sun, Y.-Z. Long, S.-L. Liu, Y.-Y. Huang, J. Ma, H.-D. Zhang, G. Shen and S. Xu, *Nanoscale*, 2013, **5**, 7041-7045.
9. M. Park, J. Im, M. Shin, Y. Min, J. Park, H. Cho, S. Park, M.-B. Shim, S. Jeon, D.-Y. Chung, J. Bae, J. Park, U. Jeong and K. Kim, *Nat Nanotechnol*, 2012, **7**, 803-809.
10. C. Merlini, G. M. O. Barra, T. M. Araujo and A. Pegoretti, *RSC Adv*, 2014, **4**, 15749-15758.
11. A. H. Najafabadi, A. Tamayol, N. Annabi, M. Ochoa, P. Mostafalu, M. Akbari, M. Nikkhah, R. Rahimi, M. R. Dokmeci, S. Sonkusale, B. Ziaie and A. Khademhosseini, *Adv. Mater.*, 2014, **26**, 5823-5830.
12. X. Lin, D. Tang, Z. Yu and Q. Feng, *J Mater Chem B*, 2014, **2**, 651-658.
13. D. Wang, T. Liu, J. Yin and S. Liu, *Macromolecules*, 2011, **44**, 2282-2290.
14. A. Zhuk, R. Mirza and S. Sukhishvili, *Acs Nano*, 2011, **5**, 8790-8799.
15. W. Gao, Q. Zhang, P. Liu, S. Zhang, J. Zhang and L. Chen, *RSC Adv*, 2014, **4**, 34460-34469.
16. X. H. Wang, X. P. Qiu and C. Wu, *Macromolecules*, 1998, **31**, 2972-2976.
17. Y. J. Zhang, S. Furyk, D. E. Bergbreiter and P. S. Cremer, *J. Am. Chem. Soc.*, 2005, **127**, 14505-14510.

18. X. L. Zhao, X. B. Ding, Z. H. Deng, Z. H. Zheng, Y. X. Peng and X. P. Long, *Macromol. Rapid Commun.*, 2005, **26**, 1784-1787.
19. X. L. Zhao, X. B. Ding, Z. H. Deng, Z. H. Zheng, Y. X. Peng, C. R. Tian and X. P. Long, *New J. Chem.*, 2006, **30**, 915-920.
20. M. Chen, M. Dong, R. Havelund, V. R. Regina, R. L. Meyer, F. Besenbacher and P. Kingshottt, *Chem. Mater.*, 2010, **22**, 4214-4221.
21. W.-J. Chuang and W.-Y. Chiu, *Polymer*, 2012, **53**, 2829-2838.
22. P. Muthiah, S. M. Hoppe, T. J. Boyle and W. Sigmund, *Macromol. Rapid Commun.*, 2011, **32**, 1716-1721.
23. Y.-J. Kim, M. Ebara and T. Aoyagi, *Adv. Funct. Mater.*, 2013, **23**, 5753-5761.
24. W.-J. Chuang, W.-Y. Chiu and H.-J. Tai, *J. Mater. Chem.*, 2012, **22**, 20311-20318.
25. L. Li, D. Yu, L. Wang and W. Wang, *J. Appl. Polym. Sci.*, 2012, **124**, 1912-1918.
26. W. Wang, Y. Jiang, S. Wen, L. Liu and L. Zhang, *J. Colloid Interface Sci.*, 2012, **368**, 241-249.
27. F. El-Tantawy, *Eur. Polym. J.*, 2002, **38**, 567-577.
28. X. Wang, S. Li, Z. Wan, Z. Quan and Q. Tan, *Int. J. Pharm.*, 2014, **463**, 81-88.

TOC



The electrical resistance of electrospun P(NIPAm-co-NMA)/Ag fibers exhibits a high sensitivity to the change of temperature around the LCST of the polymer, making them promising candidates for flexible sensors.